Geophysical Research Letters

RESEARCH LETTER
10.1029/2021GL094908

Key Points:

- Wildfire emissions contribute 23% of surface PM2.5 concentration in the contiguous United States during the summer of 2020
- Wildfires were the primary contributor to the 3,720 exceedances of National Ambient Air Quality Standard for PM2.5 during the 2020 summer
- Our finding highlights the predominating influence of wildfires on air quality during the 2020 wildfire season

Supporting Information:

Supporting Information may be found in the online version of this article.

Correspondence to:

Y. Li and D. Tong,
yli74@gmu.edu;
qtong@gmu.edu

Citation:

Li, Y., Tong, D., Ma, S., Zhang, X., Kondragunta, S., Li, F., & Saylor, R. (2021). Dominance of wildfires impact on air quality exceedances during the 2020 record-breaking wildfire season in the United States. *Geophysical Research Letters*, *48*, e2021GL094908. https://doi.org/10.1029/2021GL094908

Received 24 JUN 2021
Accepted 11 OCT 2021

Dominance of Wildfires Impact on Air Quality Exceedances During the 2020 Record-Breaking Wildfire Season in the United States

Yunyao Li[1], Daniel Tong[1,2], Siqi Ma[1], Xiaoyang Zhang[3], Shobha Kondragunta[4], Fangjun Li[3], and Rick Saylor[5]

[1]Department of Atmospheric, Oceanic and Earth Sciences, George Mason University, Fairfax, VA, USA, [2]Center for Spatial Information Science and Systems, George Mason University, Fairfax, VA, USA, [3]Geospatial Sciences Center of Excellence, Department of Geography & Geospatial Sciences, South Dakota State University, Brookings, SD, USA, [4]NOAA Satellite Meteorology and Climatology Division, College Park, MD, USA, [5]NOAA Air Resources Laboratory, College Park, MD, USA

Abstract The western United States experienced a record-breaking wildfire season in 2020. This study quantifies the contribution of wildfire emissions to the exceedances of health-based National Ambient Air Quality Standard (NAAQS) for fine particles ($PM_{2.5}$) by comparing two CMAQ simulations, with and without wildfire emissions. During August to October 2020, western wildfires contributed 23% of surface $PM_{2.5}$ in the contiguous US (CONUS), with a larger contribution in Pacific Coast (43%) and Mountain Region (42%). Consequently, wildfires were the primary contributor to the 3,720 observed exceedances. The wildfire influence peaked on September 14th, 2020, when 273 exceedances were recorded and wildfire emissions contributed 41%, 81%, and 72% to surface $PM_{2.5}$ concentrations in the CONUS, Pacific Coast, and Mountain Region, respectively. Our finding highlights the predominating influence of wildfires on air quality, and potentially human health, that is expected to grow with increasing fire activities, while anthropogenic emissions decrease.

Plain Language Summary In the summer of 2020, the western United States experienced a record-breaking number of wildfires. We looked into the effects of these wildfires on air quality, through the lens of the exceedances of health-based National Ambient Air Quality Standards (NAAQS) for fine particles ($PM_{2.5}$), which are associated with the bulk of health risks posed by air pollution. We found that in 2020, the western wildfires contributed 23% of surface $PM_{2.5}$ pollution during August to October in the contiguous United States. The contribution is much bigger in the Pacific Coast (43%) and the Mountain Region (42%). Consequently, the wildfires were the primary contributor to the 3,720 exceedances of $PM_{2.5}$ NAAQS. Our finding highlights the dominating influence of wildfire emissions on air quality and potentially on human health.

1. Introduction

Biomass burning (BB) emits a large quantity of aerosols and trace gases into the atmosphere, often leading to hazardous air quality and health problems (Koning, et al., 1985). In the summer of 2020, the western United States experienced a record-breaking wildfire season. A series of large wildfires, fueled by accumulated biomass, heatwaves, and dry winds, burned more than 10.2 million acres. These wildfires spread rapidly and destroyed several small towns in California, Oregon, and Washington. According to MODIS (Moderate Resolution Imaging Spectroradiometer) measured FRP (fire radiative power) from 2002 to 2020 (Figure 1a), the monthly total FRP in September 2020 (big red dot) over the contiguous United States (CONUS) is the highest in over the past 19 years and is more than twice as large as the second highest. Dense wildfire smoke also produced hazardous air quality that affected millions of people in major cities for weeks. Based on Suomi NPP VIIRS (Visible Infrared Imaging Radiometer Suit) 550 nm aerosol optical depth (AOD) measurements, the fire smoke was transported across the continent to the eastern U. S. coast via the westerlies in the middle of September (Figure 1b).

Previous studies (Cascio, 2018; C. E. Reid et al., 2016) demonstrated that a strong association exists between exposure to wildfire smoke and all-cause mortality and respiratory morbidity. Strong positive associations

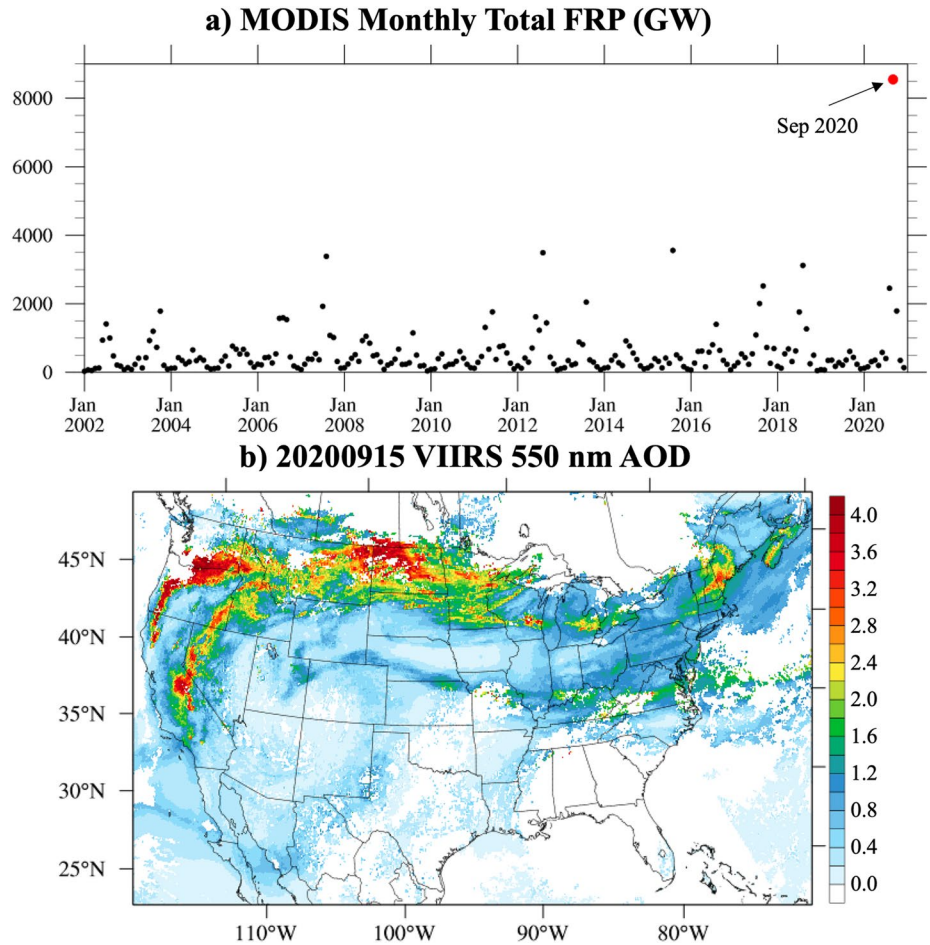

Figure 1. (a) MODIS measured monthly total FRP (GW) over the US from January 2002 to September 2020; (b) VIIRS measured 550 nm AOD on September 15, 2020.

are present between wildfire smoke exposure and exacerbations of asthma, chronic obstructive pulmonary disease, bronchitis and pneumonia. Johnston et al. (2012) found that the global average annual mortality attributable to landscape fire smoke exposure was 339,000 deaths annually. O'Neill et al. (2021) discussed the regional health impacts from the 2017 Northern California wildfires. Estimated mortality attributable to $PM_{2.5}$ exposure during the smoke episode was 83 with 47% attributable to wildfire smoke. Liu et al. (2021) assess the health impact of 2020 Washington State wildfire smoke episode which causes 38.4 more all-causes mortality cases and 15.1 more respiratory mortality cases.

To protect human health and the environment, the National Ambient Air Quality Standards (NAAQS) have been established for seven criteria air pollutants (CAPs), which includes carbon monoxide (CO), ozone (O_3), particulate matter (PM), nitrogen dioxide (NO_2), and sulfur dioxide (SO_2) that can be emitted or formed by biomass burning. Among these CAPs, $PM_{2.5}$ (PM with aerodynamic diameter of 2.5 micrometers or less) is of particular concern. The Global Burden of Disease comparative risk assessment attributed 3.2 million premature deaths worldwide to human exposure to ambient $PM_{2.5}$ in 2010, which is much greater than other air pollutants or some well-known health threats (e.g., malaria, HIV-AIDS, etc.) (Lim et al., 2012). Currently, the U.S. Environmental Protection Agency (EPA) has primary and secondary standards for $PM_{2.5}$ (annual average standards with levels of 12.0 and 15.0 $\mu g/m^3$, respectively; 24-hr standards with 98th percentile forms and levels of 35 $\mu g/m^3$) (U.S. EPA, 2020a). The EPA also employs the Exceptional Events Rule for unusual or naturally occurring events (i.e., wildfire, high wind dust events, etc.), so that air quality data influenced by these sources can be excluded to determine exceedances of NAAQS.

This study aims to assess the air quality impact of the record-breaking wildfires in 2020, with a focus on exceedances of the NAAQS for $PM_{2.5}$. We use the George Mason University (GMU) wildfire forecast system (Section 2.2) that relies on satellite estimates of biomass burning emissions and the Community Multi-scale Air Quality Modeling System (CMAQ) to simulate emission, transport, and transformation of smoke $PM_{2.5}$ during the 2020 summer wildfire season. The prediction and evolution of wildfire plumes and their impact on air quality is very challenging due to large uncertainties in wildfire emissions (Pan et al., 2020; Pereir et al., 2016), estimation of plume rise (Briggs, 1969; Freitas et al., 2007; Paugam et al., 2016; Rio et al., 2010; Sofiev et al., 2012; Stein et al., 2009; Vernon et al., 2018; Zhu et al., 2018), meteorological fields, and chemical transport processes (F. Li et al., 2019; Y. Li et al., 2020). The BB emissions product used in this study is the blended Global Biomass Burning Emissions Product from MODIS and VIIRS (GBBEPx V3, Zhang et al., 2012, 2019). To enhance the modeling system's capability to predict wildfire smoke, we have implemented a new plume rise scheme based on the algorithm proposed by Sofiev et al. (2012) into the CMAQ model. The current plume rise scheme in CMAQ is based on Briggs (1969), which was originally designed for simulating plumes from well-defined sources such as power plants in a non-disturbed atmosphere. The Sofiev scheme utilizes fire radiative power (FRP), planetary boundary layer (PBL) height, and the Brunt-Vaisala frequency in the free troposphere to estimate fire injection height. Both the Sofiev plume rise scheme and the GBBEPx emission products have been shown to perform well during large wildfire events such as the 2018 Camp Fire (Y. Li et al., 2020).

2. Methods and Data

2.1. Experiment Design

To evaluate the impact of wildfires on air quality, three CMAQ simulations were conducted. In the first run (ALLF), all emissions from wildfires, prescribed fires, and other biomass burning sources are accounted for in the model simulation. In the second run with no fire emissions (NOF), all types of biomass burning emissions are excluded. The third run (WDF) is the same as the ALLF run, but only has western (west of 102°W) U.S. wildfire emissions. In the WDF run, the USGS 24-category land use categories are used to define the location of forests (i.e., deciduous broadleaf forest, deciduous needleleaf forest, evergreen broadleaf, evergreen needleleaf, and mixed forest).

Comparing results from these three simulations will elucidate the impacts of biomass burning, wildfire, and prescribed fires on air quality. The impacts of biomass burning are computed by subtracting the NOF results from ALLF. Wildfire emission impact is represented by the difference between WDF and NOF, and the impacts from prescribed fires and other burning sources aside from wildfires are illustrated by the difference between ALLF and WDF.

2.2. Description of the Modeling System

The CMAQ model is a numerical air quality model that simulates the concentration of airborne gases and particles and the deposition of these pollutants. CMAQ V5.3.1 (U.S. EPA, 2020b) was employed to simulate the 2020 summer wildfire season from August 1st to October 31st, over the contiguous United States (CONUS) domain. Details about the system setup are shown in Table S1 in Supporting Information S1. The model resolution is 12 km with 35 vertical layers. The 12 km Weather Research and Forecasting (WRF; Skamarock et al., 2019) model V4.2 output was used as the meteorology inputs for the CMAQ model. The initial and boundary conditions for WRF are from the Global Data Assimilation System (GDAS) 0.25-degree analysis and forecast. The time step for the simulation was 60 s. The main physics choices were the Grell-Freitas scheme (Grell & Freitas, 2014) for parameterized cumulus processes, the Mellor-Yamada-Janjic scheme (Janjic, 1994) for the planetary boundary layer (PBL) processes, the two-moment Morrison microphysics (Morrison et al., 2009) for cloud physics processes, the RRTMG scheme (Iacono et al., 2008) for longwave and shortwave radiation, and the Noah scheme (Koren et al., 1999) for land surface processes.

The initial chemistry conditions on August 1st are from the NOAA operational air quality forecast (https://airquality.weather.gov/). Anthropogenic emissions of nitrogen oxides (NO_x), volatile organic compounds (VOCs), sulfur dioxide (SO_2), carbon monoxide (CO), ammonia (NH_3), and particulate matter were prepared via the 2016v1 Emissions Modeling Platform (Eyth et al., 2020). The base year of the emission inventory used

in this platform is National Emissions Inventory (NEI) 2016v1. We then shifted the base year emission to the prediction year 2020 on the basis of representative days of each month. (U.S. EPA, 2020c). The model-ready emission files are processed and generated by the Sparse Matrix Operator Kernel Emissions (SMOKE) model (Houyoux et al., 2000) V4.7. The CB6 gas-phase chemical mechanism (Luecken et al., 2019), AE07 aerosol scheme (Pye et al., 2015; Xu et al., 2018), and aqueous chemistry (Fahey et al., 2017) are used in the CMAQ system.

2.3. Biomass Burning Emissions and Plume Rise Treatment

Prior studies suggest large differences among fire emission data sets (Y. Li et al., 2020; Pan et al., 2020) and plume rise schemes (Briggs, 1969; Freitas et al., 2007; Y. Li et al., 2020; Sofiev et al., 2012; Val Martin, et al., 2018), which affect the simulation of surface air pollution due to fires (Y. Li et al., 2020; Xie et al., 2020). Y. Li et al. (2020) compared four satellite-based fire emission datasets, including the Fire Energetics and Emissions Research algorithm (FEER, Ichoku & Ellison, 2014), Fire Locating and Monitoring of Burning Emissions (FLAMBE, J. S. Reid et al., 2009), Global Fire Assimilation System (GFAS, Kaiser et al., 2012), and GBBEPx (Zhang et al., 2012, 2014, 2019), two plume rise schemes (Briggs and Sofiev) with a dispersion model. They found that GBBEPx together with the Sofiev plume rise scheme showed the best performance among different combinations of emission datasets and plume rise algorithms. Therefore, the GBBEPx biomass burning emission data and the Sofiev plume rise scheme are used in this study.

The GBBEPx v3 system produces daily global BB emissions ($PM_{2.5}$, BC, CO, CO_2, OC, NO_x, NH_3, and SO_2) at a spatial resolution of 0.1° or 3 km based on FRP. The product blends fire observations from MODIS on the NASA Terra and Aqua satellites, VIIRS on the Suomi National Polar-orbiting Partnership (SNPP) and Joint Polar Satellite System (JPSS-1). Specifically, BB emissions from MODIS are calculated using the same algorithm as Quick Fire Emissions Data set (QFED) (Darmenov & da Silva, 2015). BB emissions from VIIRS are converted directly from VIIRS FRP using a set of coefficients that are derived between VIIRS FRP and QFED emissions. The GBBEPx v3 emissions are the average of MODIS and VIIRS emissions estimates. Overall GBBEPx v3 is comparable to QFED, but it provides more fire detections spatially and temporally.

To achieve a better simulation of fire plumes, the Sofiev et al. (2012) plume rise scheme was implemented into the CMAQ model. The Sofiev scheme utilizes FRP, PBL height (H_{PBL}), and the Brunt-Vaisala (BV) frequency in the free troposphere to estimate the plume injection height (H_p) for wild-land fires:

$$H_p = \alpha H_{\mathrm{PBL}} + \beta\left(\frac{\mathrm{FRP}}{\mathrm{FRP}_0}\right)^{\gamma} \exp\left(-\frac{\delta \mathrm{BV}_{\mathrm{FT}}^2}{\mathrm{BV}_0^2}\right) \quad (1)$$

where FRP is the daily fire radiative power provided in NOAA GBBEPx V3, $FRP_0$is the reference fire power which equals to 106 W, BV_{FT} is the Brunt-Vaisala frequency in the free troposphere (FT), BV_0 is the reference Brunt-Vaisala frequency which equals to 2.5×10^{-4} s^{-2}, and where α, β, γ, δ, are constants. The α, β, γ, δ values are based on Sofiev et al. (2012), and Y. Li et al. (2020). For wildfire simulations, the Sofiev scheme is more stable and accurate (Y. Li et al., 2020) than the CMAQ default plume rise scheme, which is the Briggs (1969) scheme designed for chimneys. Figure S1 in Supporting Information S1 compares the CMAQ simulated plume top with Multi-angle Imaging SpectroRadiometer (MISR) Plume Height observation (Val Martin et al., 2010) for the Complex fire that happened on August 31, 2020. The simulated plume top is comparable to the observation.

2.4. Observation Data and Assessment Method

To evaluate the model simulation as well as the wildfire emission impacts, the simulated results are compared to AirNow ground $PM_{2.5}$ observations and VIIRS measured AOD at 550 nm.

The area hit ratio (Kang et al., 2007) is used to evaluate the surface $PM_{2.5}$ simulation. The calculation of area hit is based on observed and simulated $PM_{2.5}$ exceedance. According to EPA NAAAQS (U.S. EPA, 2020a), the exceedance level (E) for $PM_{2.5}$ is set to 35 $\mu g/m^3$ for 24-hr $PM_{2.5}$. Area hit (aH) is defined as:

$$aH = \left(\frac{E_{\mathrm{OM}}}{E_{\mathrm{OM}} + E_O} \right) \tag{2}$$

where E_{OM} is the number of exceedances that are both observed and simulated in the 5 × 5 grid cells centered at the monitor location (Kang et al., 2007). E_O is the number of observed exceedances that are not simulated within the 5 × 5 grid cells centered at the monitor location.

The Contribution Ratio (CR) and Exceedance Impact Ratio (EIR) are used to discuss the wildfire biomass burning influence:

$$\mathrm{CR} = \frac{M_{\mathrm{WDF}} - M_{\mathrm{NOF}}}{M_{\mathrm{WDF}}} \times 100\% \tag{3}$$

$$\mathrm{EIR} = \frac{N_{\mathrm{aff}}}{N_{\mathrm{tot}}} \times 100\% \tag{4}$$

where M_{WDF} is the simulation results (i.e., $PM_{2.5}$, AOD) from the WDF (wildfire only) run, M_{NOF} is the result from the NOF (no fire) run, N_{tot} is the number of total grid cells within the study region (i.e., CONUS, different time zones), and N_{aff} is the number of grid cells that are within the unhealthy wildfire-influenced area in the study region. The unhealthy wildfire-influenced area is defined as the place where the simulated 24-hr $PM_{2.5}$ levels from the WDF run is higher than the exceedance level (35 $\mu g/m^3$) and the simulated 24-hr $PM_{2.5}$ from the NOF run is lower than the exceedance level over the same location.

3. Results

3.1. Model Evaluation

The first exceedance of the daily $PM_{2.5}$ NAAQS (24-h $PM_{2.5}$ concentration higher than 35 $\mu g/m^3$) occurred on August 16th, 2020. After October 10th, wildfire emissions began to decrease, with less than 10 exceedances after that date. Therefore, the analysis focuses on the period from August 16th to October 10th, 2020. Figure 2a shows the result of the area hit ratio (blue line) for the CMAQ ALLF run. A high area hit ratio represents a good capture of the region impacted by real smoke. The average area hit ratio during this period is 0.68. During the peak pollution days (from September 12th to 16th) when over 200 stations observed $PM_{2.5}$ exceedance (black dash line in Figure 2), the area hit ratios were higher than 0.96 with a maximum of 1.0 on September 13th, 2020. This suggests that the model could predict more than 96% of the observed exceedances when the smoke pollution was at its peak. The minimum area hit ratio was 0 on August 17th, 2020; however, there were no intense fires and there were only three stations that observed $PM_{2.5}$ exceedances on that day. Traditional evaluation metrics are also used to evaluate the model simulation. The correlation between observed and simulated daily $PM_{2.5}$ concentrations for the ALLF run is shown in Figure 2a (red line) with an average of 0.55. The averaged normalized mean error of GMU-CMAQ simulated surface $PM_{2.5}$ is 3.9% for the year of 2020. The spatial plot of ALLF $PM_{2.5}$ overlaid by AirNow observations on a peak day is shown in Figure 2b. The contour colors are based on the EPA Air Quality Index for $PM_{2.5}$: green for good, yellow for moderate, orange for unhealthy to sensitive groups, red for unhealthy, purple for very unhealthy, and maroon for hazardous. In most places, the observations and simulation match closely with each other, suggesting that the model performs very well. The AOD results are shown in Figure 2c. Our model reproduced the smoke optical depth from the west coast to the east coast observed by VIIRS (Figure 1b), but the magnitude was slightly lower than VIIRS in Oregon and North Dakota. The simulated $PM_{2.5}$ cross sections in the Western Coast and Central U.S. was compared with Cloud-Aerosol Lidar and Infrared Pathfinder Satellite Observations (CALIPSO) in Figure S2 in Supporting Information S1. The simulated vertical distribution of the smoke matched the observation near the wildfire source region and downwind area. Overall, the model is able to reproduce wildfire smoke dispersion, especially when the fire is intense.

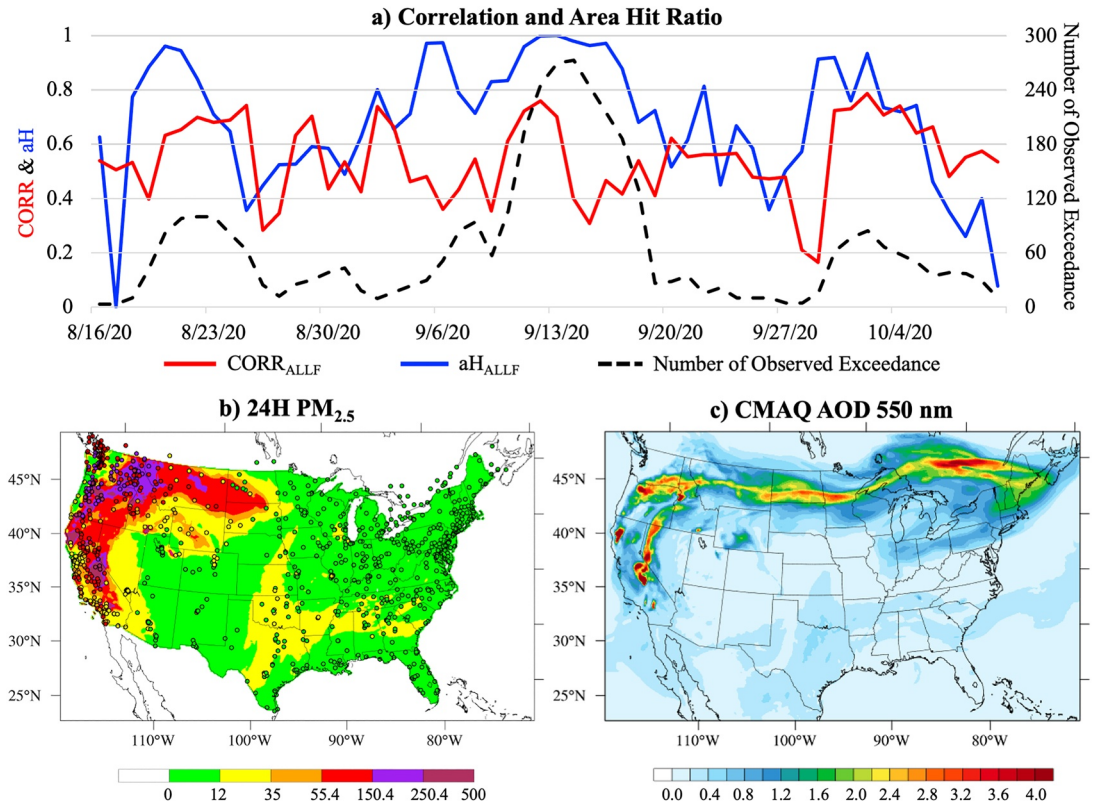

Figure 2. (a) Correlation (red) and area hit ratio (blue) between observed and simulated $PM_{2.5}$ from the ALLF run, with the number of observed exceedances (black dash line) from August 16th to October 31st, 2020; (b) CMAQ ALLF run for simulated 24-h $PM_{2.5}$ and overlaid with the AirNow $PM_{2.5}$ observation on September 15th, 2020; (c) CMAQ ALLF run for simulated AOD at 550 nm on September 15th, 2020.

3.2. Wildfire Contribution to $PM_{2.5}$ and AOD

Figure 3a illustrates the contribution from wildfires to surface $PM_{2.5}$ concentration in the four different time zone regions in the CONUS. (Figure S3 in Supporting Information S1), including Pacific time zone (hereafter Pacific Coast), Mountain time zone (hereafter Mountain Region), Central time zone (hereafter Central Region), and Eastern time zone (hereafter Eastern Coast). During the analysis period, the West Coast wildfires contributed 23% of surface $PM_{2.5}$ pollution nationwide. Specifically, wildfires produced 43% of the total $PM_{2.5}$ pollutants in the Pacific Coast, 42% in the Mountain Region, 11% in the Central Region, and 4% in the Eastern Coast. The $PM_{2.5}$ difference between the WDF run and the NOF run and the wildfire $PM_{2.5}$ CR on September 15, 2020 (one of the peak days) are shown in Figures 3c and 3e. During the peak period, the wildfire $PM_{2.5}$ CRs reached 41% nationwide, 81% in the Pacific Coast, 72% in the Mountain Region, 33% in the Central Region, and 10% in the Eastern Coast.

The thick smoke that originated from California, Oregon, and Washington was transported across the country by the prevailing westerly wind. During September 14–17th, 2020, the fire smoke from the West Coast was transported to the northeastern part of the U.S. (Figures 1b and 2c). While the fire smoke traveled east, it passed 19 states, which included California, Nevada, Oregon, Washington, Idaho, Montana, Wyoming, North Dakota, South Dakota, Minnesota, Wisconsin, Michigan, Pennsylvania, New York, Connecticut, Rhode Island, Massachusetts, Vermont, New Hampshire, and Maine. The smoke plume was still optically thick when it reached New Hampshire and Maine and had a measured AOD of over 3.

Figure 3b shows the contribution of wildfire emissions to AOD during the study period. The western wildfires contributed an average of 32% to nationwide AOD, 45% in the Pacific Coast, 45% in the Mountain Region, 26% in the Central Region, and 14% in the Eastern Coast. On peak days, the wildfire contributed more than 60% of the AOD nationwide, 80% in the Pacific Coast, 80% in the Mountain Region, 60% in the Central Region, and 50% in the Eastern Coast. Although the increased AOD resulting from aloft smoke does

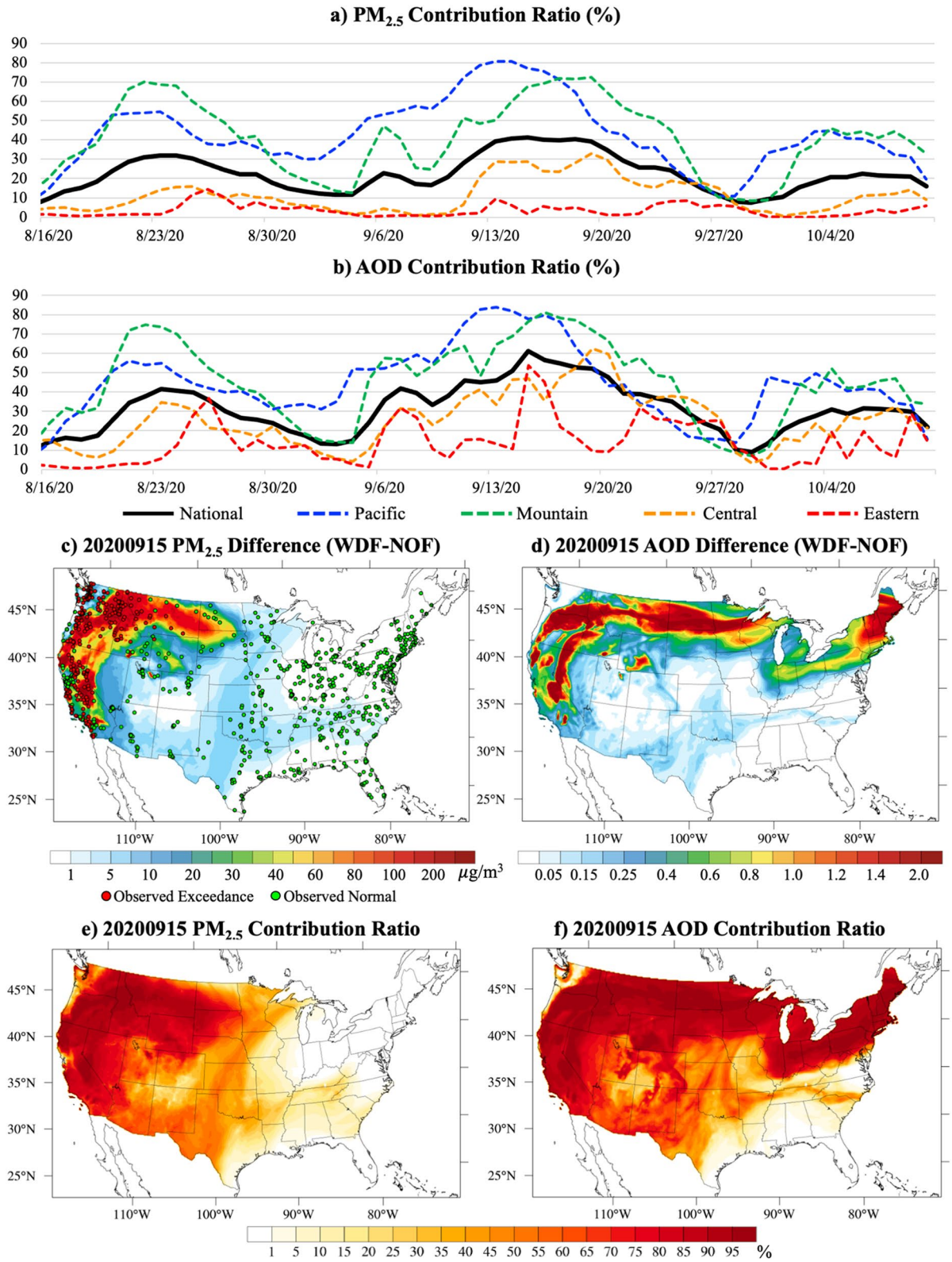

Figure 3. Wildfire $PM_{2.5}$ (a) and AOD (b) contribution ratios; simulation differences between WDF and NOF run on September 15th, 2020, for $PM_{2.5}$ (c, overlaid with observed $PM_{2.5}$ exceedances) and AOD (d); and the wildfire $PM_{2.5}$ (e) and AOD (f) contribution ratio on September 15, 2020.

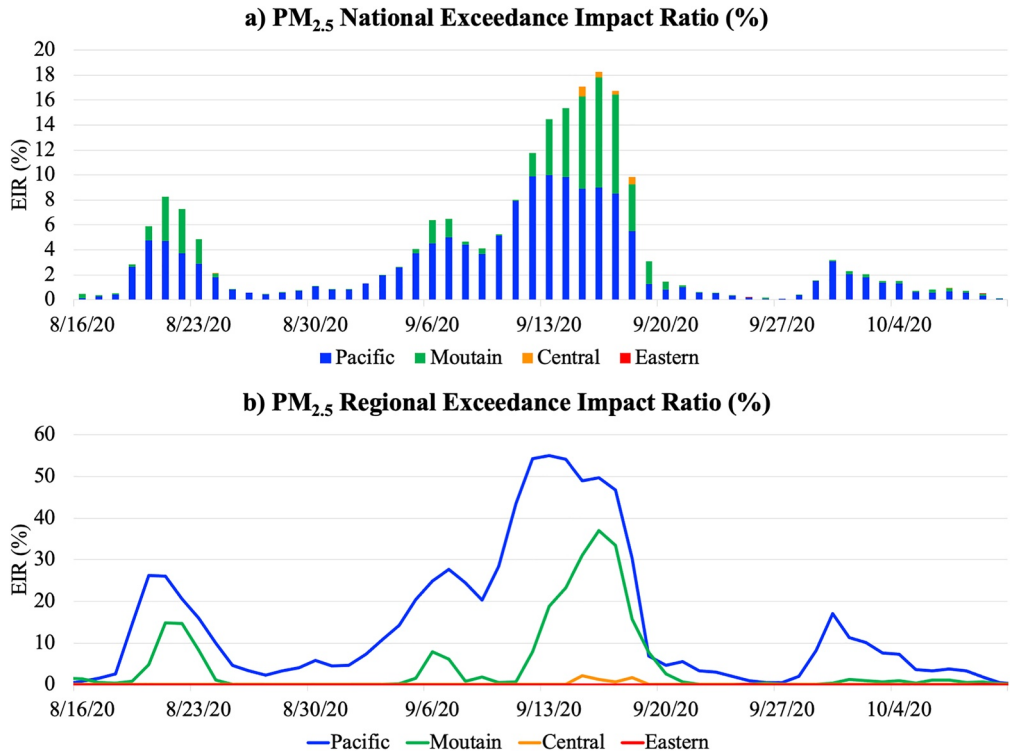

Figure 4. National (a) and Regional (b) wildfire $PM_{2.5}$ Exceedance Impact Ratio (%).

not have the severe health impacts of surface $PM_{2.5}$, it influences a larger area than surface $PM_{2.5}$ and may affect cloud formation and regional radiative budgets, leading to impacts on regional weather. Nevertheless, in July 2021, the wildfire smoke from northwest Ontario, Canada reached the U.S. East Coast. The smoke plume has touched down to the surface, causing a widespread air pollution episode. The impact of the 2021 wildfire will be discussed in the following paper.

3.3. Impacts of Air Quality Exceedance Caused by Wildfires

According to AirNow ground observations, there were 3,720 observed $PM_{2.5}$ exceedances during the analysis period, with an average of 65 exceedances per day and a maximum of 273 exceedances on September 14th, 2020. The observed unhealthy air ($PM_{2.5}$ exceedances, red circles in Figure 3c) crossed seven states in the western U.S., including California, Nevada, Oregon, Washington, Idaho, Montana, and Wyoming. The CMAQ simulations show that the surface smoke might also have extended to the region without ground measurements, such as North Dakota and South Dakota (Figure 3c). The $PM_{2.5}$ exceedances are all located in the areas with large simulated $PM_{2.5}$ differences between the WDF and NOF runs, which indicates that all the observed $PM_{2.5}$ exceedances are caused by wildfire emissions rather than other emissions, such as prescribed burning or other anthropogenic emissions.

The results for wildfire $PM_{2.5}$ national Exceedance Impact Ratio (EIR, Equation 4) are shown in Figure 4a. During the peak period, over 18% of surface area nationwide was blanketed in the unhealthy air caused by wildfire smoke. About half of the affected region was located in the Pacific Coast region, and the other half in the Mountain Region. Only a few areas in the Central Region or Eastern Coast were affected by the surface $PM_{2.5}$ exceedances. The wildfire $PM_{2.5}$ regional EIR for the four time zones are shown in Figure 4b. More than half of the Pacific Coast and one third of the area in the Mountain Region experienced surface $PM_{2.5}$ exceedances.

4. Conclusion

In the summer of 2020, the Western United States experienced a record-breaking wildfire season, with the highest FRP in September 2020 in the past 19 years. The CMAQ system with GBBEPx biomass burning and the newly added Sofiev plume rise scheme were used to simulate the 2020 record-breaking wildfire season. The model simulation successfully reproduced the plume dispersion. For surface $PM_{2.5}$, the average area hit ratio is 0.68, and the averaged correlation is 0.55 during the two months. More than 96% of the polluted area was successfully reproduced during the most polluted days. For AOD, our model reproduced the smoke optical depth from the west coast to the east coast observed by VIIRS, but the magnitude was slightly lower than VIIRS in Oregon and North Dakota.

From late August to early October, the West Coast wildfires contributed 23% of surface $PM_{2.5}$ pollution nationwide. More than 40% of the $PM_{2.5}$ pollution came from the western wildfires (the Pacific Coast and Mountain Region). During the peak days, the wildfire contribution to surface $PM_{2.5}$ reached 81% in the Pacific Coast, 72% in the inter-Mountain region, and 41% across the entire country. Even in the Eastern Coast, which is far away from the source region, the model estimates that there is 10% of the total $PM_{2.5}$ pollution came from the West Coast wildfires.

The thick fire smoke that originated in California, Oregon, and Washington was injected into the free troposphere and transported across the country through the prevailing wind, which caused hazy days in 19 states. On the peak days, more than 60% of the nationwide AOD was caused by wildfire emissions. Specifically, 80% in the Pacific Coast and Mountain Region, 60% in the Central Region, and 50% AOD in the Eastern Coast were attributed to wildfire plumes. Although the increased AOD caused by the aloft smoke did not have severe health impacts compared to surface $PM_{2.5}$, it influenced a larger area than surface $PM_{2.5}$ and might have further influence on cloud formation and earth radiative budget, which would impact regional weather as well as global climate.

Finally, the West Coast wildfires caused 3,720 observed $PM_{2.5}$ exceedances during the analysis period, with an average of 65 exceedances per day, and a maximum of 273 exceedances on September 14, 2020. The observed unhealthy air ($PM_{2.5}$ exceedances based on the EPA AirNow observations) crossed seven states in the western United States. The surface smoke may also extend to regions where there are no ground measurements in North Dakota and South Dakota based on our CMAQ simulation. During the peak days, over 18% of the CONUS was blanketed by the unhealthy air caused by wildfire smoke. Following research will be conducted on exploring the impacts of wildfire pollution on human health.

Data Availability Statement

The MISR data used in this paper can be found here: http://air.csiss.gmu.edu/yli/paper_data/MISR. The GBBEPx data can be downloaded from https://satepsanone.nesdis.noaa.gov/pub/FIRE/GBBEPx-V3/. The VIIRS measurements can be downloaded from http://air.csiss.gmu.edu/yli/paper_data/viirs/. The AirNow observations can be downloaded from: https://files.airnowtech.org/?prefix=airnow/2020/. The GDAS 0.25-degree analysis and forecast data can be download from https://rda.ucar.edu/datasets/ds083.3/. The CALIPSO plots can be found here: https://www-calipso.larc.nasa.gov/tools/data_avail/. The CMAQ results can be download from: http://air.csiss.gmu.edu/yli/paper_data/.

Acknowledgments
This work was financially supported by the NOAA Weather Program Office and office of Oceanic and Atmospheric Research (OAR), NASA Health and Air Quality Program, and George Mason University College of Science. The authors thank Dr. Ralph Kahn for providing us the MISR plume height measurements.

References

Briggs, G. (1969). *Plume rise: A critical review* (Technical Report). (p. 81). Springfield, VA: National Technical Information Service.

Cascio, W. E. (2018). Wildland fire smoke and human health. *Science of the Total Environment*, *624*, 586–595. https://doi.org/10.1016/j.scitotenv.2017.12.086

Darmenov, A., & da Silva, A. (2015). *The Quick Fire Emissions Dataset (QFED)—Documentation of Versions 2.1, 2.2 and 2.4* (Vol. 38). NASA Global Modeling and Assimilation Office. Retrieved From https://gmao.gsfc.nasagov/pubs/docs/Darmenov796.pdf

Eyth, A., Vukovich, J., Farkas, C., & Strum, M. (2020). *Technical Support Document (TSD) preparation of emissions inventories for 2016v1 North American emissions modeling platform*.

Fahey, K. M., Carlton, A. G., Pye, H. O. T., Baek, J., Hutzell, W. T., Stanier, C. O., et al. (2017). A framework for expanding aqueous chemistry in the Community Multiscale Air Quality (CMAQ) model version 5.1. *Geoscientific Model Development*, *10*, 1587–1605. https://doi.org/10.5194/gmd-10-1587-2017

Freitas, S. R., Longo, K. M., Chatfield, R., Latham, D., Silva Dias, M. A. F., Andreae, M. O., et al. (2007). Including the sub-grid scale plume rise of vegetation fires in low resolution atmospheric transport models. *Atmospheric Chemistry and Physics*, *7*(13), 3385–3398. https://doi.org/10.5194/acp-7-3385-2007

Grell, G. A., & Freitas, S. R. (2014). A scale and aerosol aware stochastic convective parameterization for weather and air quality modeling. *Atmospheric Chemistry and Physics*, *14*(10), 5233–5250. https://doi.org/10.5194/acp-14-5233-2014

Houyoux, M., Vukovich, J., Brandmeyer, J. E., Seppanen, C., & Holland, A. (2000). *Sparse matrix operator kernel emissions modeling system-SMOKE User manual*. Research Triangle Park, NC: MCNC-North Carolina Supercomputing Center, Environmental Programs.

Iacono, M. J., Delamere, J. S., Mlawer, E. J., Shephard, M. W., Clough, S. A., & Collins, W. D. (2008). Radiative forcing by long-lived greenhouse gases: Calculations with the AER radiative transfer models. *Journal of Geophysical Research*, *113*, D13103. https://doi.org/10.1029/2008JD009944

Ichoku, C., & Ellison, L. (2014). Global top-down smoke-aerosol emissions estimation using satellite fire radiative power measurements. *Atmospheric Chemistry and Physics*, *14*(13), 6643–6667. https://doi.org/10.5194/acp-14-6643-2014

Janjić, Z. I. (1994). The Step-Mountain Eta Coordinate Model: Further developments of the convection, viscous sublayer, and turbulence closure schemes. *Monthly Weather Review*, *122*(5), 9272–945. https://doi.org/10.1175/1520-0493(1994)122<0927:TSMECM>2.0

Johnston, F., Henderson, S., Chen, Y., Randerson, J., Marlier, M., DeFries, R., et al. (2012). Estimated global mortality attributable to smoke from landscape fires. *Environmental Health Perspectives*, *120*(5), 695–701. https://doi.org/10.1289/ehp.1104422

Kaiser, J. W., Heil, A., Andreae, M. O., Benedetti, A., Chubarova, N., Jones, L., et al. (2012). Biomass burning emissions estimated with a global fire assimilation system based on observed fire radiative power. *Biogeosciences*, *9*(1), 527–554. https://doi.org/10.5194/bg-9-527-2012

Kang, D., Mathur, R., Schere, K., Yu, S., & Eder, B. (2007). New categorical metrics for air quality model evaluation. *Journal of Applied Meteorology and Climatology*, *46*(4), 549–555. https://doi.org/10.1175/jam2479.1

Koning, H. W., Smith, K. R., & Last, J. M. (1985). Biomass fuel combustion and health. *Bulletin of the World Health Organization*, *63*(1), 11–26.

Koren, V., Schaake, J., Mitchell, K., Duan, Q.-Y., Chen, F., & Baker, J. M. (1999). A parameterization of snowpack and frozen ground intended for NCEP weather and climate models. *Journal of Geophysical Research*, *104*, 19585–19569. https://doi.org/10.1029/1999JD900232

Li, F., Val Martin, M., Andreae, M. O., Arneth, A., Hantson, S., Kaiser, J. W., et al. (2019). Historical (1700–2012) global multi-model estimates of the fire emissions from the Fire Modeling Intercomparison Project (FireMIP). *Atmospheric Chemistry and Physics*, *19*(19), 12545–12567. https://doi.org/10.5194/acp-19-12545-2019

Li, Y., Tong, D. Q., Ngan, F., Cohen, M. D., Stein, A. F., Kondragunta, S., et al. (2020). Ensemble PM2.5 forecasting during the 2018 Camp Fire event using the HYSPLIT transport and dispersion model. *Journal of Geophysical Research: Atmospheres*, *125*, e2020JD032768. https://doi.org/10.1029/2020JD032768

Lim, S., Vos, T., Flaxman, A. D., Danaei, G., Shibuya, K., Adair-Rohani, H., et al. (2012). A comparative risk assessment of burden of disease and injury attributable to 67 risk factors and risk factor clusters in 21 regions, 1990–2010: A systematic analysis for the Global Burden of Disease Study 2010. *Lancet*, *380*, 2224–2260.

Liu, Y., Austin, E., Xiang, J., Gould, T., Larson, T., & Seto, E. (2021). Health impact assessment of the 2020 Washington State wildfire smoke episode: Excess health burden attributable to increased PM2.5 exposures and potential exposure reductions. *GeoHealth*, *5*, e2020GH000359. https://doi.org/10.1029/2020gh000359

Luecken, D. J., Yarwood, G., & Hutzell, W. H. (2019). Multipollutant of ozone, reactive nitrogen and HAPs across the continental US with CMAQ-CB6. *Atmospheric Environment*, *201*, 62–72. https://doi.org/10.1016/j.atmosenv.2018.11.060

Morrison, H., Thompson, G., & Tatarskii, V. (2009). Impact of cloud microphysics on the development of trailing stratiform precipitation in a simulated squall line: Comparison of one- and two-moment schemes. *Monthly Weather Review*, *137*(3), 991–1007. https://doi.org/10.1175/2008MWR2556.1

O'Neill, S. M., Diao, M., Raffuse, S., Al-Hamdan, M., Barik, M., Jia, Y., et al. (2021). A multi-analysis approach for estimating regional health impacts from the 2017 Northern California wildfires. *Journal of the Air & Waste Management Association*, *71*(7), 791–814. https://doi.org/10.1080/10962247.2021.1891994

Pan, X., Ichoku, C., Chin, M., Bian, H., Darmenov, A., Colarco, P., et al. (2020). Six global biomass burning emission datasets: Inter-comparison and application in one global aerosol model. *Atmospheric Chemistry and Physics*, *20*(2), 969–994. https://doi.org/10.5194/acp-20-969-2020

Paugam, R., Wooster, M., Freitas, S., & Val Martin, M. (2016). A review of approaches to estimate wildfire plume injection height within large-scale atmospheric chemical transport models. *Atmospheric Chemistry and Physics*, *16*, 907–925. https://doi.org/10.5194/acp-16-907-2016

Pereir, G., Siqueira, R., Rosário, N., Longo, K., Freitas, S. R., Cardozo, F. S., et al. (2016). Assessment of fire emission inventories during the South American Biomass Burning Analysis (SAMBBA) experiment. *Atmospheric Chemistry and Physics*, *16*, 6961–6975. https://doi.org/10.5194/acp-16-6961-2016

Pye, H. O. T., Luecken, D. J., Xu, L., Boyd, C. M, Ng, N. L., Baker, K. R., et al. (2015). Modeling the current and future roles of particulate organic nitrates in the southerneastern United States. *Environmental Science & Technology*, *49*(24), 14195–14203. https://doi.org/10.1021/acs.est.5b03738

Reid, C. E., Brauer, M., Johnston, F. H., Jerrett, M., Balmes, J. R., & Elliott, C. T. (2016). Critical review of health impacts of wildfire smoke exposure. *Environmental Health Perspectives*, *124*, 1334–1343. https://doi.org/10.1289/ehp.1409277

Reid, J. S., Hyer, E. J., Prins, E. M., Westphal, D. L., Zhang, J., Wang, J., et al. (2009). Global monitoring and forecasting of biomass-burning smoke: Description of and lessons from the Fire Locating and Modeling of Burning Emissions (FLAMBE) Program. *IEEE Journal of Selected Topics in Applied Earth Observations and Remote Sensing*, *2*(3), 144–162. https://doi.org/10.1109/JSTARS.2009.2027443

Rio, C., Hourdin, F., & Chédin, A. (2010). Numerical simulation of tropospheric injection of biomass burning products by pyro-thermal plumes. *Atmospheric Chemistry and Physics*, *10*(8), 3463–3478. https://doi.org/10.5194/acp-10-3463-2010

Skamarock, W. C., Klemp, J. B., Dudhia, J., Gill, D. O., Liu, Z., Berner, J., et al. (2019). *A description of the advanced research WRF version 4* (p. 145). NCAR.

Sofiev, M., Ermakova, T., & Vankevich, R. (2012). Evaluation of the smoke-injection height from wild-land fires using remote-sensing data. *Atmospheric Chemistry and Physics*, *12*(4), 1995–2006. https://doi.org/10.5194/acp-12-1995-2012

Stein, A. F., Rolph, G. D., Draxler, R. R., Stunder, B., & Ruminski, M. (2009). Verification of the NOAA smoke forecasting system: Model sensitivity to the injection height. *Weather and Forecasting*, *24*(2), 379–394. https://doi.org/10.1175/2008WAF2222166.1

United States Environmental Protection Agency. (2020a). *Review of the National Ambient Air Quality Standards for Particulate Matter*. (pp. 82684–82748). Retrieved From https://www.govinfo.gov/content/pkg/FR-2020-12-18/pdf/2020-27125.pdf

United States Environmental Protection Agency. (2020b). *CMAQ (Version 5.3.2)*[Software]. Retrieved From https://doi.org/10.5281/zenodo.4081737

United States Environmental Protection Agency. (2020c). *Technical Support Document (TSD) Preparation of Emissions Inventories for 2016v1 North American Emissions Modeling Platform*. (pp. 120–121). Retrieved From https://www.epa.gov/sites/default/files/2020-10/documents/2016v1_emismod_tsd_508.pdf

Val Martin, M., Kahn, R., & Tosca, M. (2018). A global analysis of wildfire smoke injection heights derived from space-based multi-angle imaging. *Remote Sensing*, *10*(10), 1609. https://doi.org/10.3390/rs10101609

Val Martin, M., Logan, J. A., Kahn, R. A., Leung, F.-Y., Nelson, D., & Diner, D. (2010). Smoke injection heights from fires in North America: Analysis of 5 years of satellite observations. *Atmospheric Chemistry and Physics*, *10*, 1491–1510. https://doi.org/10.5194/ACP-10-1491-2010

Vernon, C. J., Bolt, R., Canty, T., & Kahn, R. A. (2018). The impact of MISR-derived injection height initialization on wildfire and volcanic plume dispersion in the HYSPLIT model. *Atmospheric Measurement Technique*, *11*, 6289–6307. https://doi.org/10.5194/amt-11-6289-2018

Xie, Y., Lin, M., & Horowitz, L. W. (2020). Summer PM2. 5 pollution extremes caused by wildfires over the western United States during 2017–2018. *Geophysical Research Letters*, *47*(16), e2020GL089429. https://doi.org/10.1029/2020GL089429

Xu, L., Pye, H. O. T., He, J., Chen, Y. L., Murphy, B. N., & Ng, N. L. (2018). Experimental and model estimates of the contributions from biogenic monoterpenes and sesquiterpenes to secondary organic aerosol in the southeastern United States. *Atmospheric Chemistry and Physics*, *18*, 12613–12637. https://doi.org/10.5194/acp-18-12613-2018

Zhang, X., Kondragunta, S., Da Silva, A., Lu, S., Ding, H., Li, F., & Zhu, Y. (2019). *The blended global biomass burning emissions product from MODIS and VIIRS observations (GBBEPx)*. Retrieved From https://www.ospo.noaa.gov/Products/land/gbbepx/docs/GBBEPx_ATBD.pdf

Zhang, X., Kondragunta, S., Ram, J., Schmidt, C., & Huang, H.-C. (2012). Near-real-time global biomass burning emissions product from geostationary satellite constellation. *Journal of Geophysical Research*, *117*(D14). https://doi.org/10.1029/2012JD017459

Zhang, X., Kondragunta, S., & Roy, D. P. (2014). Interannual variation in biomass burning and fire seasonality derived from geostationary satellite data across the contiguous United States from 1995 to 2011. *Journal of Geophysical Research: Biogeosciences*, *119*(6), 1147–1162. https://doi.org/10.1002/2013JG002518

Zhu, L., Val Martin, M., Gatti, L., Kahn, R., Hecobian, A., & Fischer, E. (2018). Development and implementation of a new biomass burning emissions injection height scheme (BBEIH v1.0) for the GEOS-Chem model (v9-01-01). *Geoscientific Model Development*, *11*, 4103–4116. https://doi.org/10.5194/gmd-11-4103-2018